Influence of an Annealing Heat Treatment on the Microstructure, Ductility, and Corrosion Resistance of a Chromated 55 wt.% Al-Zn Coated Steel Sheet

T.M.C. Nogueira, M.A.S. Cruz, and P.R. Rios

(Submitted 9 March 2000; in revised form 5 January 2001)

The effect of an annealing heat treatment on both the ductility and corrosion resistance of a chromated hot-dip 55 mass% Al-Zn coated steel sheet is investigated. The present results suggest that the heat treatment improves coating ductility but impairs the overall corrosion resistance due to a decrease in the protective effect of the passivation layer and possibly due to the decrease in the amount of interdendritic zinc. Based on these results, it is concluded that the benefits of the heat treatment to improve ductility have to be carefully assessed with reference to the intended application due to its adverse effect on the corrosion resistance.

Keywords 55% Al-Zn coating, coated steel sheet, corrosion

1. Introduction

Hot-dip 55 wt.% Al-Zn coatings on steel sheets are obtained by a process similar to hot-dip galvanizing. The final product combines the long-term durability of aluminum and the galvanic protection of zinc, thus offering good corrosion resistance.

These coatings often undergo a passivating treatment for an additional corrosion protection during transport and storage.[1] A common passivation agent used is chromic acid, leading to a complex chromate film, which contains Cr (III) and Cr (VI) compounds.[2,3] These chromate films are normally too thin to be detected by conventional metallographic techniques, and, in this work, electrochemical techniques are used to study them.

Although the coating ductility is usually adequate, for certain more demanding applications, such as roll forming, it would be desirable to improve the ductility. It has been suggested that one can significantly improve the ductility of 55 wt.% Al-Zn coatings by an annealing heat treatment.[4–6] However, a possible inconvenience of these treatments is that they might decrease the protecting effect of the passivation.

In this work, the effect of an annealing heat treatment on both the ductility and corrosion resistance of chromated hot-dip 55 mass% Al-Zn coated steel sheets is investigated.

2. Experimental Methods and Materials

2.1 Material

Commercial 55 mass% Al-Zn coated steel sheets with and without the final surface chromatizing treatment were used. The samples had a nominal total coating weight (computing the coating weight on both sides) of 160 g/m^2 that corresponds to a coating thickness of about 20 μm. The substrate chemical analysis was (in mass%): C-0.063, Mn-0.23, P-0.008, S-0.0046, Si-0.037, N-0.0085, Al-0.037, and Fe-balance. The coating had a nominal composition of 55 mass% Al-43.5 mass% Zn-1.5 mass% Si.

2.2 Heat Treatments

Two heat-treatment temperatures, 200 and 360 °C, were used following the recommended practice for improving coating ductility.[4–6] The specimens were held at the annealing temperature for 16 h (57,600 s) under a protective nitrogen atmosphere and slowly cooled, 0.02 °C/s, in the furnace to 190 °C followed by cooling in air. All specimens were aged at room temperature for 10 days (8.64×10^5 s) prior to the mechanical testing. Optical microscopy and scanning electron microscopy (SEM) were carried out to characterize the microstructure.

2.3 Coating Ductility

The coating ductility before and after the heat treatments was compared by analyzing the cracks that appear in the coating after bending the sheet. The samples to be tested had dimensions of 200 × 10 × 0.5 mm. The samples were bent with an internal nominal diameter of 0.5 mm that corresponds to 1 T bending. The bending test was carried out in two steps: first, the samples were bent manually around a suitable former until the sheet was at an angle of approximately 30°; in the second step, the sheet was bent down to the desired radius using an Instron machine in compression so that bending would occur under controlled conditions for all samples. For each condition, 36 samples were used, as there was considerable scatter in the data.

After being bent, the samples were cut, polished, and examined in cross section in an optical microscope with image analysis equipment. The area of analysis comprised a region within a 90° arc at the tip of the bend and was examined at a magnification of 200×. The arc length was calculated by $\pi d/4$, where d was the internal bending radius. The number of cracks per

T.M.C. Nogueira, M.A.S. Cruz, and **P.R. Rios,** Universidade Federal Fluminense, Escola de Engenharia Industrial Metalúrgica de Volta Redonda, Av. dos Trabalhadores, 420, Vila Santa Cecília, Volta Redonda, RJ, 27255-125 Brazil. Contact e-mail: prrios@metal.eeimvr.uff.br.

unit of arc length was measured. The cracks were grouped in three classes according to the extent that they crossed the coating:

- cracks that completely crossed the coating, that is, that crossed 100% of the coating thickness;
- cracks that did not completely cross the coating but that crossed half the coating thickness, that is, that crossed more than 50% but less than 95% of the coating thickness; and
- cracks that did not cross half the coating distance, that is, that crossed more that 5% but less than 50% of the coating thickness.

2.4 Corrosion Resistance

The corrosion resistance of the samples was studied by the accelerated salt spray test and by two electrochemical methods: analysis of the voltammetric dissolution curve and determination of the corrosion current density by the Tafel plots.[7]

Anodic Voltammetric Technique. The voltammetric dissolution of the coated samples (not bent) was carried out in an aqueous solution containing 0.25 M of H_2SO_4. The area of the sample was equal to 9.08 cm^2, limited by an O-ring in the polarization cell. The counter electrode was a platinum wire and the reference electrode was the normal calomel electrode. A scan rate of 0.001 V s^{-1} from an initial potential of -1 V until a final potential of $+1$ V was used for the voltammetric dissolution, and curves of current density against potential, voltammograms, or potentiometric diagrams were obtained.

In order to determine the electrochemical behavior of the main components of the 55 mass% Al-Zn coated steel sheet, a preliminary study of electrodes of pure zinc, pure aluminum, and the steel substrate in this electrolyte was carried out. From the polarization curves obtained for Zn and Al in 0.25 M of H_2SO_4 for potentials between -1.050 and -0.525 V, one can expect to be able to dissolve the 55 mass% Al-Zn coating without dissolution of the steel substrate.[8]

Tafel Plots. The anodic and cathodic polarization curves were made using the pH = 5.3 phthalate-buffered solution, with 0.5 M NaCl, in order to obtain the Tafel plots. The corrosion current densities were obtained from the extrapolation of the linear portion to overpotential equal to zero.

Salt Spray. Accelerated salt spray tests were carried out in a mist containing 5 wt.% NaCl following the standard ASTM B117.

3. Results and Discussion

Figure 1(a) and (b) show the top view of the coating in the as-received condition and after heat treatment at 360 °C, respectively. In the as-received condition, the material consisted of Al-rich dendrites surrounded by interdendritic Zn-rich regions. After the heat treatment, as can be seen in Fig. 1(b), the original dendritic structure could still be perceived, but now one can see a copious precipitation within the Al dendrites. At the heat-treatment holding temperatures, the Al-Zn equilibrium diagram[1] shows that there is significant solid solubility of Zn in Al. Therefore, during the heat treatment, a certain degree of homogenization occurs. Solid-state diffusion of Zn into the dendrites and of Al into the interdendritic regions takes place. As a consequence, the Al dendrites become enriched in Zn. As the temperature decreases during the slow cooling step of the heat treatment, the excess Zn forms coarse Zn-rich precipitates within the Al dendrites. Thus, the result of the heat treatment is a decrease in the amount of interdendritic Zn with a corresponding appearance of Zn-rich precipitates within the Al dendrites.

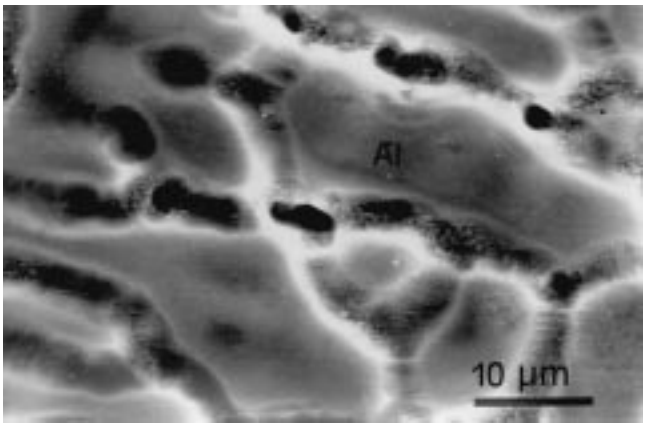

(**a**)

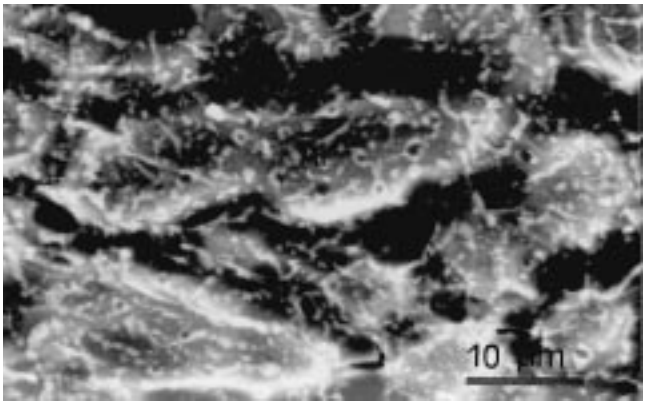

(**b**)

Fig. 1 SEM micrographs, top view, of a 55% Al-Zn coating before bending: (**a**) as received, a precipitate-free Al dendrite is marked in the figure; and (**b**) heat treated at 360 °C, an Al dendrite marked in the figure now shows copious Al-Zn precipitation. Compare the marked regions in the two micrographs

Figure 2(a) and (b) show the appearance of the as-received coating after the 1 T bend test. Large cracks, almost parallel to the bend axis, can be seen close to the specimen tip (Fig. 2a). In Fig. 2(b), a less deformed region can be seen, slightly off the specimen tip. The cracks, some of them indicated by arrows in Fig. 2(b), start at the interdendritic regions.

Table 1 contains the results of the measurements of the number of cracks caused by the bending as a function of heat treatment. Previous work[5,6] has considered only those cracks that crossed the entire coating thickness, that is, cracks that crossed 100% of the coating thickness. When one compares only cracks that crossed 100% of the coating thickness, it is clear that the heat treatment brought about a significant reduction in

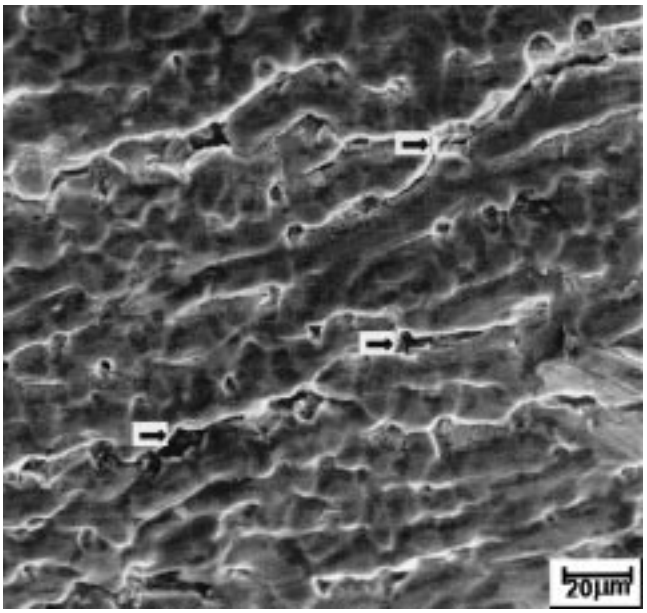

(**a**)

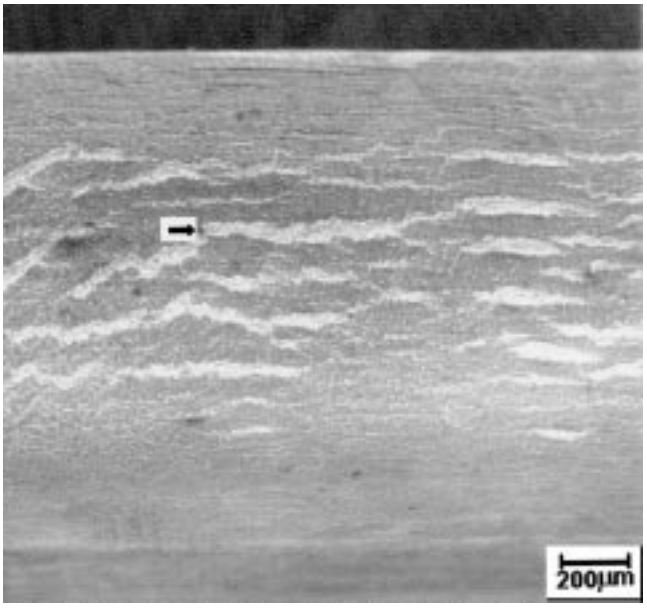

(**b**)

Fig. 2 SEM micrographs, top view, of a 55% Al-Zn as-received coating after 1 T bending: (**a**) general view: large cracks, one of them indicated by an arrow, develop at the tip of the bent specimen parallel to the bend axis (direction of arrows); and (**b**) detail from a region slightly off the tip of the bent specimen: cracks indicated by arrows can be seen to start at the interdendritic regions

the number of cracks observed in the coating. The heat treatment carried out at 200 °C was particularly successful in this regard: in the as-received condition, one had 18 cracks/mm, whereas in the specimen heat treated at 200 °C, one could find only 2 cracks/mm. The heat treatment carried out at 360 °C also improved the coating ductility, though to a somewhat lesser extent: one obtained 10 cracks/mm. So the present results are in broad agreement with previous work.[5,6] Nonetheless, one observes an interesting difference between the as-received and the heat-treated material. Whereas the former only has cracks that crossed 100% of the coating thickness, the latter also had a population of shorter cracks, as shown in Table 1. When one includes the number of shorter cracks, the total number of cracks becomes comparable for the three conditions. Willis[5] proposed that cracks nucleated at the interdendritic regions (Fig. 2b) associated with Si flakes that probably remain unchanged by the heat treatment. The fact that a comparable total number of cracks were found suggests that the nucleation of the cracks was not greatly affected by the heat treatment, which is consistent with Willis'[5] suggestion. It appears that the main effect of the heat treatment was to arrest crack growth. As a consequence, although the total number of cracks was comparable in all three conditions, the number of cracks that crossed 100% of the coating thickness was clearly less for the heat-treated samples when compared with the as-received sample. One can infer that, although there was an improvement in coating ductility with the heat treatments, as demonstrated by the crack arrest, the improvement in ductility might not be as large as it appears from comparing only the cracks that crossed 100% of the coating thickness, since the present results suggest that crack nucleation is probably less affected by the heat treatment than by crack growth.

The results of the salt spray test can be found in Table 2. The effect of the heat treatment is clear. The corrosion resistance of the heat-treated specimens as evidenced by visible corrosion products was significantly worse than the corrosion resistance of the as-received specimen. Moreover, the material treated at the highest heat-treating temperature had the worst corrosion resistance. It is not easy to tell to what extent this was caused by the effect of heat treatment on the microstructure or by somehow decreasing the effect of the passivation treatment. In any case, the net result of the heat treatment was to decrease the corrosion resistance.

The salt spray results were confirmed by the corrosion current densities, which are shown in Table 3. It is clear that the corrosion current density was substantially increased by the heat treatments.

The potentiometric diagrams, obtained by a DC anodic voltammetric technique, are shown in Fig. 3(a) to (c) for the as-received and heat-treated at 200 and 360 °C chromated samples, respectively. The anodic dissolution voltammetric technique applied to coatings containing several phases may present peaks that correspond to the dissolution of the individual phases. In order to obtain such peaks and also to make sure that minimum overlap occurs between them, a careful choice of the electrolyte and scanning rate is necessary.[8,9] As shown in Fig. 3, the effect of the heat treatment on the potentiometric diagrams is remarkable. For the as-received chromated sample, the potentiometric diagram showed only a small current density due to a very strong protecting effect of the passivation treatment. For the heat-treated samples, well-defined peaks corresponding to zinc dissolution can be observed (Fig. 3b and c). However, when one compares a chromated as-received specimen with a chromated heat-treated one, two effects are observed together: the effect of the microstructural change and the effect of the heat treatment on the chromate layer itself. In order to isolate the effect of the heat treatment, potentiometric diagrams of nonchromated samples were obtained and are shown in Fig. 4.

Table 1 Number of cracks in the 55% Al-Zn chromated coating caused by the 1 T bending test as a function of coating heat-treating temperature

	As received		Heat treated at 200 °C		Heat treated at 360 °C	
	Cracks/mm	% of total number of cracks	Cracks/mm	% of total number of cracks	Cracks/mm	% of total number of cracks
<50% of coating thickness	…	…	11 ± 2	65	11 ± 1	41
>50% but <100% of coating thickness	…	…	4 ± 1	23	6 ± 1	22
>100% of coating thickness	18 ± 2	100	2 ± 1	12	10 ± 2	37
Total	18	100	17	100	27	100

Table 2 Salt spray tests of 55% Al-Zn chromated coating: W—white corrosion, and R—red corrosion

Annealing time (s)	As received	Heat treated at 200 °C	Heat treated at 360 °C
1.44×10^4	…	Traces of W	Traces of W
1.8×10^6	10% W	100% W	100% W
3.6×10^6	30% W	100% W	100% W + traces of R
6.1×10^6	65% W	100% W + 25% R	100% W + 70% R

Table 3 55% Al-Zn chromated coating corrosion current densities (mA/cm^2) obtained from Tafel plots as a function of heat-treatment temperature

As received	Heat treated at 200 °C	Heat treated at 360 °C
0.001	0.016	0.050

In Fig. 4(a), the potentiometric diagram of the as-received sample exhibits a well-defined peak related to Zn dissolution, compared with Fig. 3(a), in which such a peak is absent due to the protection afforded by the passivating layer. The zinc peak significantly decreases as the temperature of the heat treatment increases (Fig. 4a to c). This reduction is a consequence of the decrease in the amount of interdendritic Zn due to the homogenization during the heat treatment. Comparing Fig. 3(b) and 4(b) and 3(c) and 4(c), one can see, comparing the values of the current densities, that the Zn peaks are significantly smaller in the chromated samples. This means that the chromate layer partially "survives" the heat treatment. In other words, the current densities in the potentiometric diagrams of the chromated samples are smaller than those of the nonchromated samples, even after heat treatment. However, this residual passivation decreases as the heat-treating temperature increases, and it is comparatively small after heat treating at 360 °C.

The present results suggest that the heat treatments change the electrochemical behavior for two reasons: (1) they "destroy" the protecting effect afforded by the passivation layer; and (2) they decrease the amount of interdendritic zinc, which results in a smaller Zn dissolution peak. The present results shows that the short-term corrosion resistance due to the passivating layer is compromised by the heat treatment. On the other hand, the effect of the heat treatment on the amount of interdendritic zinc could have long-term implications, as the coating is dependent on the zinc for cathodic protection. It is not easy to separate these two effects in practice, but the overall corrosion resistance of the coating in salt spray tests and inferred from Tafel plots showed that the heat-treated samples had a poorer corrosion resistance.

4. Summary and Conclusions

The present results showed that heat treating the 55% Al-Zn coating can improve its ductility. With the methodology followed here, a heat treatment at 200 °C gave the most significant improvement. When only the cracks that crossed 100% of the coating thickness were compared, as is usual in this sort of study, the effect was indeed strong. However, when the population of short cracks was included, the increase in ductility was somewhat less impressive, as the total number of cracks was comparable for all three conditions investigated. It is suggested that the heat treatment had a less significant effect on crack nucleation in contrast with the significant effect on the crack growth within the Al-Zn coating.

The present work also shows that the heat treatment impairs the overall corrosion resistance due to a decrease in the protecting effect of the passivation layer and possibly due to the decrease in the amount of interdendritic zinc.

In conclusion, the present results suggest that the benefits of the heat treatment to improve ductility have to be carefully assessed with reference to the intended application due to its adverse effect on the corrosion resistance.

Acknowledgments

This work was partially supported by Companhia Siderúrgica Nacional (CSN) through an agreement with Universidade Federal Fluminense (UFF). M.A.S. Cruz is grateful to CSN for the scholarship. This work is part of a project partly funded by Financiadora de Estudos e Projetos—FINEP. P.R. Rios is also grateful to Conselho Nacional de Desenvolvimento Científico e Tecnológico (CNPq) for the financial support. Thanks are extended to Professor G. Ferran for helpful discussions and useful suggestions. The authors also thank Professor I. de S.

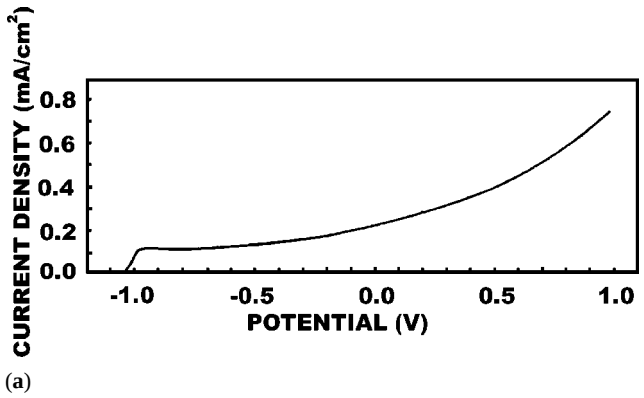

(**a**)

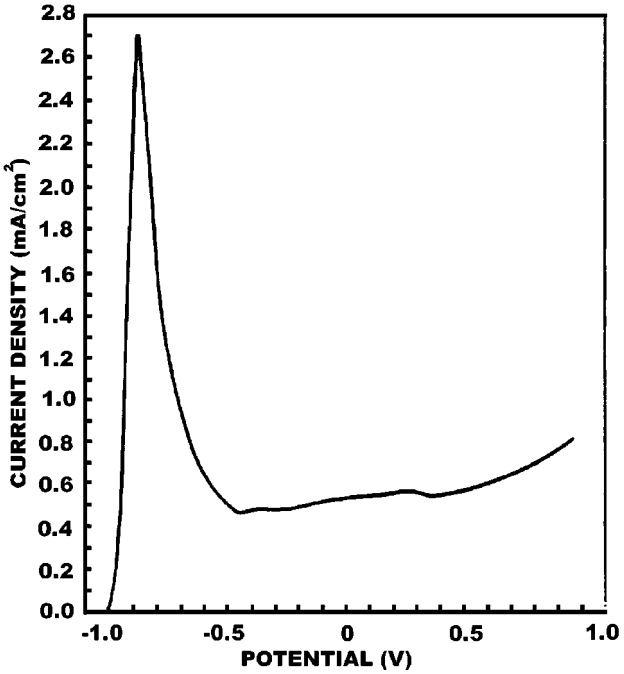

(**b**)

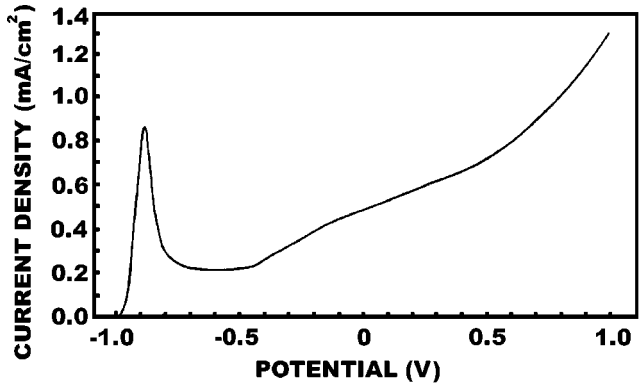

(**c**)

Fig. 3 Potentiometric diagrams of a chromated 55 wt.% Al-Zn coating in H_2SO_4: (**a**) as received, (**b**) heat treated at 200 °C, and (**c**) heat treated at 360 °C

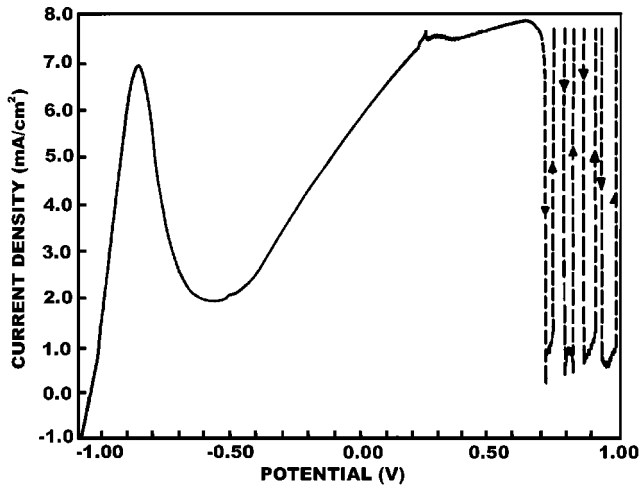

(**a**)

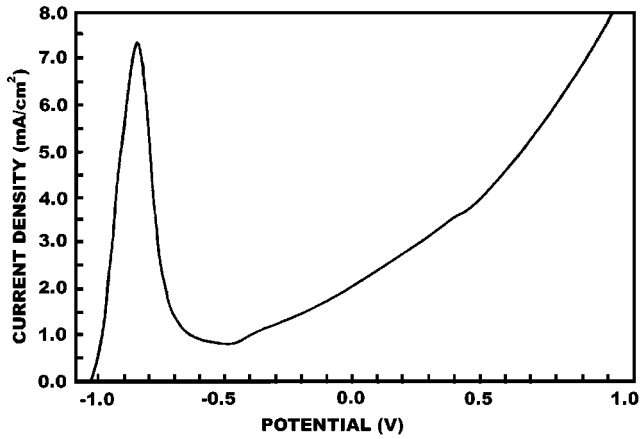

(**b**)

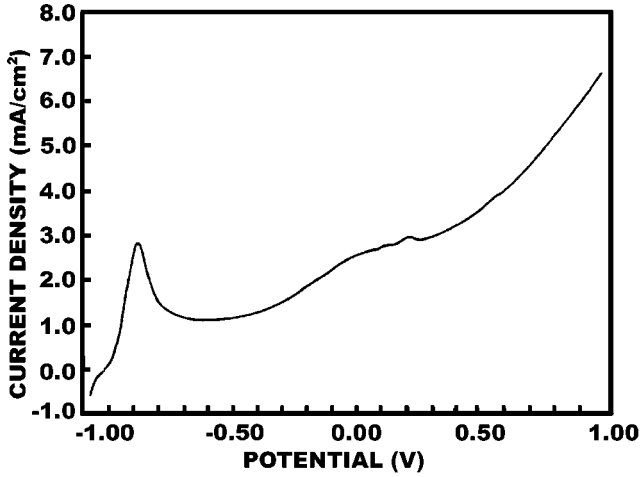

(**c**)

Fig. 4 Potentiometric diagrams of a nonchromated 55 wt.% Al-Zn coating in H_2SO_4: (**a**) as received, (**b**) heat treated at 200 °C, and (**c**) heat treated at 360 °C

Bott for help with the SEM at Pontifícia Universidade Católica do Rio de Janeiro.

References

1. F. Porter: *Zinc Handbook*, Marcel Dekker, Inc., New York, NY, 1991.
2. H.E. Townsend and J.C. Zoccola: *J. Electrochem. Soc. Solid-State Sci. Technol.*, 1978, vol. 125 (8), pp. 1290-92.
3. H.E. Townsend and R.G. Hart: *J. Electrochem. Soc. Solid-State Sci. Technol.*, 1984, vol. 131 (6), pp. 1345-48.
4. L.K. Allegra, H.E. Towsend, and A.R. Borzillo: U.S. Patent 4,287,009, Sept. 1, 1981.
5. D.J. Willis: *Proc. Int. Conf. on Zinc and Zinc Alloy Coated Steel Sheet (Galvatech)*, Yoshihiro Hisamatsu, ed., The Iron and Steel Institute of Japan, Tokyo, 1989, pp. 351-58.
6. D.J. Willis and Z.F. Zhou: *Proc. Int. Conf. Zinc and Zinc Alloy Coated Steel Sheet (Galvatech)*, The Iron and Steel Society, Chicago, IL, 1995, pp. 455-62.
7. A.J. Bard and L.R. Faulkner: *Electrochemical Methods*, John Wiley and Sons, New York, NY, 1980.
8. T.M.C. Nogueira, M.A.S. Cruz, and P.R. Rios: *Iron Steel Inst. Jpn. Int.*, 1999, vol. 39, pp. 295-97.
9. T.M.C. Nogueira, U.R. Seixas, and P.R. Rios: *Iron Steel Inst. Jpn. Int.*, 1998, vol. 38, pp. 775-77.